JOURNAL OF MATERIALS SCIENCE 10 (1975) 314–320

Hot-pressing behaviour of silicon carbide powders with additions of aluminium oxide

F. F. LANGE
Materials Science Section, Metallurgy and Metals Processing Department, Westinghouse Research Laboratories, Pittsburgh, Pennsylvania, USA

The hot-pressing behaviour of different silicon carbide powders (average particle sizes ranging from $\sim$ 0.5 to 9 μm) with aluminium oxide additions ranging from 0.01 to 0.15 volume fractions was investigated. Using powders with an average particle size < 3 μm, densities $\geq 99\%$ theoretical could be achieved at 1950° C (1 h) with 28 MN m^{-2} for volume fractions of $Al_2O_3 \geq 0.02$. A liquid phase forms at high temperatures which dissolves the silicon carbide particles to promote densification by a solution-reprecipitation mechanism.

1. Introduction

Alliegro *et al.* [1] were the first to recognize that silicon carbide powders (either the cubic, β-phase or the poly-type, hexagonal, α-phase) could be densified under pressure with the aid of an additive. Their extensive study of different hot-pressing aids suggested that aluminium (either in elemental form or as an oxide) would result in a high density ($> 98\%$ of theoretical)* material.

Because the role of this additive is not understood and silicon carbide is a leading candidate for high temperature structural application, an investigation was undertaken to obtain a more basic understanding of the hot-pressing behaviour of this material. In particular, it was of interest to determine the conditions that lead to densification, the role of the additive during densification and the effect of the fabrication parameters on the resulting microstructure, which in turn, can control the mechanical properties.

2. Experimental

2.1. Starting powders

Five different powders were examined which were designated 600 RA,† 1200 RA,† 1500 RA,† EK‡, and PPG.§ Most studies were performed with the EK and PPG powders. The particle size distribution was measured with an instrument¶ that assumed Stoke's relation for the settling of spherical shaped particles. As shown in Fig. 1, their average particle sizes are: 600 RA, 9 μm; 1200 RA, 5 μm; 1500 RA, 3.5 μm; and EK, 2 μm. The manufacturer of the PPG powder reported a surface area of 11 to 16 $m^2 g^{-1}$; thus its average particle size is < 0.5 μm. With the aid of a microscope, the PPG powder was found to contain occasional large (> 30 μm), hard aggregates. These were identified by the manufacturer as non-stoichiometric SiC aggregates [2].

Table I reports the major cation impurities in these powders determined by qualitative spectrographic emission. The impurities reported for the 1500 RA powder are typical of the Carborundum powders (600 RA and 1200 RA). In addition, the manufacture of the EK powder reported free Si: 0.15 wt %, free C: 1.4 wt %, and SiO_2: 2.2 wt %. Likewise, the PPG powder was reported to contain an average of 1.2% excess C. A neutron activation analysis (courtesy of Dr H. Priest, AMMRC) of the 1500 RA powder showed 0.9 wt % oxygen which could indicate the presence of $\sim$ 2 wt % SiO_2. It was presumed that all the powders contained a SiO_2 surface layer due to handling in air ambients.

Table I also reports the crystal phase of these powders as determined by X-ray analysis. The 600 RA, 1200 RA, 1500 RA and EK powders

*Theoretical density of silicon carbide is 3.22 g cm^{-3}.
†Carborundum, Niagara Falls, N.Y.
‡Electroschrmelzwerk, Germany.
§PPG Industries, Pittsburgh, Pa.
¶Micromeritics.

TABLE I Crystal phase and cation impurity content of silicon carbide powders

		Cation impurities (wt %)												
Powder*	Phase	Al	B	Ca	Cr	Cu	Fe	Mg	Mn	Nb	Ni	Ti	V	Zr
1500 RA	$\alpha+\beta$	0.08	—	0.003	0.002	0.001	0.05	0.005	—	0.005	0.01	0.06	0.03	0.05
EK	$\alpha+\beta$	0.1	0.05	0.01	—	—	0.03	0.002	—	—	—	0.06	0.02	0.02
PPG	β	—	0.007	—	0.007	0.002	0.05	—	0.01	—	0.02	0.005	—	—

1500 RA: Carborundum, EK: Electroschremelzwerk, Germany, PPG: PPG Industries.

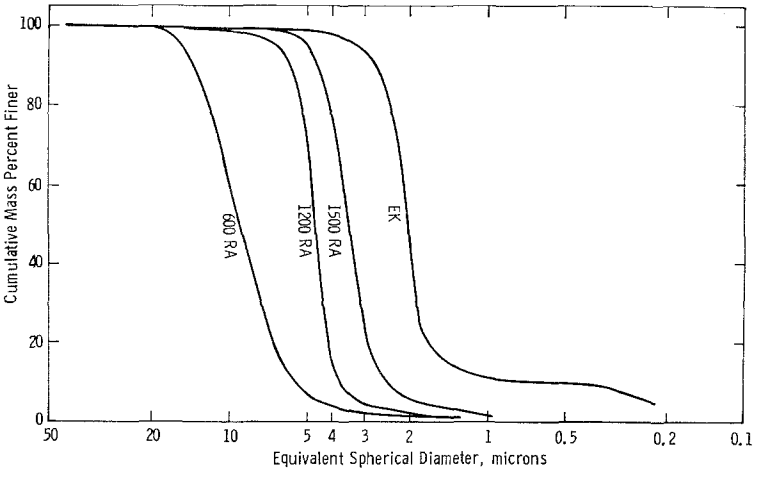

Figure 1 Particle size distribution of four of the five powders used in the investigation.

were a mixture of hexagonal poly-types (α-phase) with some minor amounts of cubic phase (β-phase). The PPG powder was cubic.

2.2. Additive and powder preparation

Linde B* Al_2O_3 powder reported to have an average particle size of 0.05 μm was used as the hot-pressing aid. Amounts corresponding to 0.01, 0.02, 0.05, 0.75, 0.10, 0.12 and 0.15 volume fractions were mixed into selected SiC powders by milling for 16 h in a plastic bottle containing tungsten carbide balls and methanol. Details are reported elsewhere [3]. Approximately 1.5 to 2.5 wt % (< 0.01 volume fraction) tungsten carbide and 1 to 2 wt % plastic contaminated the powder. The milled slurry was mixed with plastic beaters during drying to prevent segradation. As reported elsewhere [3] milling reduced the average particle size by $\sim$ 50%. Occasional large aggregates were still found in the milled PPG powder.

2.3. Hot-pressing

Discs slightly less than 2 in. diameter were pre-pressed at 70 MN m^{-2} resulting in green densities between 45 and 55% of theoretical depending on the starting powder. Graphfoil* was used to separate the discs from the 2 in. i.d. graphite die and end plungers. A hot-press† with induction heating was used for densification. Temperature was measured with an optical pyrometer through two different glass viewing ports, each aligned with a drilled hole in the graphite die-susceptor. Each resulted in the same measurement at temperatures $\geqq$ 1800°C. Compaction was recorded (within $\pm$ 0.002 in) by measuring the ram movement with the aid of a linear resistor.

*Union Carbide Corporation.
†Vacuum Industries, Sommerville, Ma.

TABLE II Limiting condition for hot-pressing SiC powders at 28 MN m^{-2} (pressure schedules I and II)

Powder	Al_2O_3 Volume fraction	Temperature (°C)	Period (h)	Density (%)
PPG	0.02	1950-2050*	1	> 99
EK	0.02-0.15	≥ 1950, ≤ 2100	1	> 99
EK	0.02	2200	2	98
1200 RA	0.02	1950	4	85
1200 RA	0.02	1950	1	94
600 RA	0.02	1975	1	66
EK	0.01	1950	1	93
EK	0.01	2025	2	94
1500 RA	0.01	2025		95

*Experiments with pressure schedules I or II were not conducted above 2050°C with this powder.

Three different pressure schedules were used.

Schedule I. A pressure of 28 MN m^{-2} was applied to the powder compact at room temperature and then released to 7 MN m^{-2}. The temperature was then rapidly raised (~ 1 h from room temperature to 1800°C to within ~ 150°C of the hot-pressing temperature. Pressure was then applied in increments of 7 MN m^{-2} to obtain 28 MN m^{-2} during the last period of temperature rise. After holding the temperature and pressure constant for a given period, the pressure was released and the furnace was shut off. Vacuum (~ 1 Torr at 1800 to 2000°C) and nitrogen (1 atm at room temperature) ambiences were used.

Schedule II. A pressure of 28 MN m^{-2} applied at room temperature, was held constant during densification.

Schedule III. Kinetic studies were performed with selected silicon carbide powders containing 0.02 volume fraction of Al_2O_3 which were heated to the desired temperature (between 1800 and 2075°C) in a nitrogen ambience. A pressure of 28 MN m^{-2} was quickly applied at the desired temperature. Compaction data were recorded as a function of time at constant applied pressure.

After cooling and sandblasting, the density of the discs were obtained by water immersion and by size-weight measurements. The compaction data were used to back-calculate the density, porosity and other necessary parameters required for data analysis.

2.4. Microstructure observations

Many of the materials were polished, etched and examined with an optical microscope and a scanning electron microscope to determine grain size and to observe second phases. An etching procedure of ~ 7 min in a boiling solution consisting of one part saturated $K_3Fe(CN)_6$ and one part saturated NaOH [4] was preferred over the electrolytic etching techniques since grain boundaries exhibited more contrast relative to the multicoloured grains usually produced with the latter technique. Grain size measurements were performed on × 5000 SEM micrographs (three areas for each material), in which each area was divided by the number of grains counted. The diagonals of the unit squares were taken as the grain size.

Attempts were made to identify second phase inclusions with a non-dispersive X-ray attachment on the SEM and with an electron microprobe. Hot-pressed specimens were ground and X-rayed to determine the crystal form of the silicon carbide and second phases.

3. Densification results

3.1. General

Table II summarizes the general results indicating that (a) the PPG and EK powders, which were used for most of the experiments, plus 0.02 VF Al_2O_3 could be densified (> 99%) within the temperature range of 1950 to 2100°C and a pressure of 28 MN m^{-2} within a period of 1 h using pressure schedules I or II; (b) large particle size powders (e.g. 1200 RA) required either longer periods at 1950°C or higher temperatures; and (c) 0.01 VF Al_2O_3 did not result in full densification for the conditions studied. Similar results were obtained for both vacuum and nitrogen ambients. Densification versus temperature relations were obtained for powders containing 0.02 VF Al_2O_3 subjected to pressure schedule II and heated at a rate of

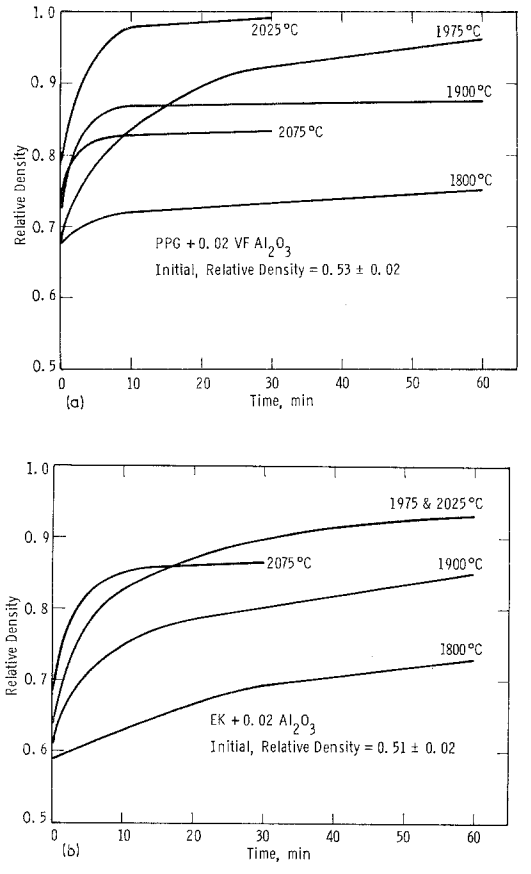

Figure 2 Relative density versus time for (a) PPG and (b) EK powders containing 0.02 VF Al_2O_3 densified at different temperatures with a pressure of 28 MN m^{-2}.

$\sim$ 5°C min^{-1} (between 1500 and 2000°C). These data showed that compaction would initiate at lower temperatures for smaller particle-size powders, namely, PPG: $\sim$ 1750°C, EK: $\sim$ 1800°C, and 1200 RA: $\sim$ 1850°C.

3.2. Kinetics

Pressure schedule III was used to investigate the rate of densification for the PPG and EK powders, each containing 0.02 VF Al_2O_3, within the temperature range of 1800 to 2075°C. These data are shown in Fig. 2 as relative density versus time. Approximately 50 to 60% of the total compaction occurred during the initial moments of pressure application (not shown in Fig. 2). Once 28 MN m^{-2} was reached, the data indicate that two stages of densification, namely, an initial period of rapid densification followed by a period of slower kinetics. When these data are analysed according to the plastic deformation model suggested by Murray *et al.* [5], i.e. by plotting the logarithm of relative porosity versus time, the final stage, which began at $\sim$ 80% of theoretical density, was characterized by a linear curve. The slope of these linear curves showed that at temperatures $\leq$ 2025°C, the densification rate during the final stage increased with increasing temperatures. At 2075°C, very little densification occurred during the final stage resulting in a porous body. Microstructural observations showed that extensive grain growth occurred before reaching full density explaining the lower densities achieved with schedule III (pressure applied at temperature) relative to pressure schedules I and II.

4. Microstructure

4.1. X-ray analysis

After hot-pressing, an X-ray diffraction analysis revealed that the same phases were present in the milled powders, i.e. β-phase SiC (PPG powder) remained β-phase* and the mixed polytype, α-phase SiC (EK, etc. powders) remained α-phase after hot-pressing; alumina and tungsten carbide were found as minor phases.

4.2. Evidence for a liquid phase

The observation of large second phase streaks was most significant since it led to direct evidence that a liquid phase sintering mechanism was responsible for densification. The streaks frequently encompassed individual grains and grain aggregates strongly suggesting a frozen liquid. Although they appeared to meander through the matrix, their longest direction was approximately perpendicular to the hot-pressing direction. This indicated that a liquid phase was squeezed into the laminar void spaces present in the cold-pressed powder discs.†

Due to their size (up to several millimetres long and usually 10 to 15 μm wide), the second

*This analysis was only performed on material hot-pressed at 1975°C. Transformation to the α-phase should occur at higher temperatures [6].

†Laminar pockets of second phase, which appeared as streaks on polished sections, could be eliminated by minimizing the laminar void spaces in the pre-stressed powder compacts. This can be accomplished in thick discs, which are more susceptible to pressure gradients and thus laminar separation, by hot-pressing several stacked thinner discs. The streaks could also be eliminated (or minimized) by grain growth. For this case the liquid phase would redistribute to grain boundaries and triple points.

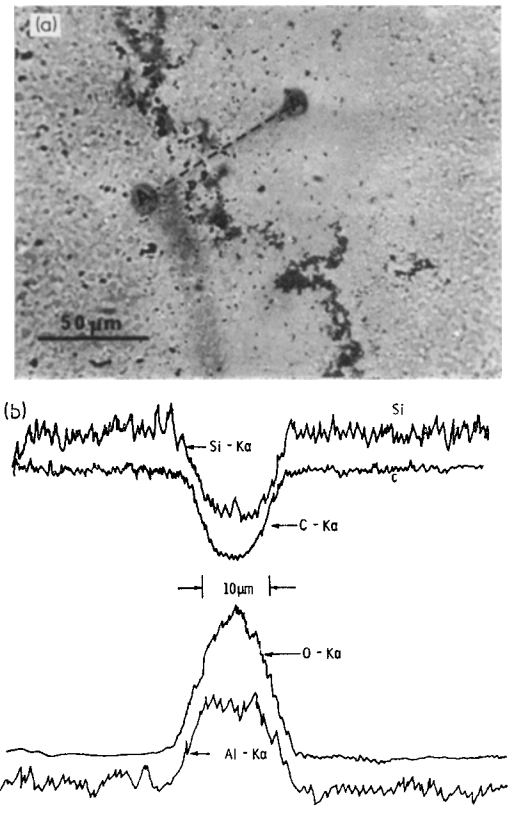

Figure 3 (a) Optical micrograph of second phase streak found in certain hot-pressed SiC bodies. Line AA is the path of the electron beam trace. Portions of the streak along this line have been obscured during tracing. (b) Intensity of Si$K\alpha$, C$K\alpha$, O$K\alpha$ and Al$K\alpha$ X-ray emissions from scanning the second phase streak illustrated in (a).

phase streaks could be analysed with the electron microprobe. Fig. 3 illustrates one of these streaks and the results of electron beam traces for the elements Al, O, Si and C showing that the streaks consisted of Al and O. The intensity gradients across the streak cannot be unambiguously interpreted as element gradients since the area of X-ray fluorescence was comparable to the streak width, i.e. part of the electron beam was always impinging on the SiC matrix as it traversed the second phase streak. Thus, these results and those of the X-ray diffraction analysis (reported above), indicate that the second phase streaks are primarily Al_2O_3.

The geometry of the interfaces between the SiC grains and the streaks show that the SiC grains were partially dissolved in the liquid phase during hot-pressing. This interface geometry can be seen more clearly in Fig. 4, which is a micrograph of a polished and etched surface of a silicon carbide material hot-pressed with 0.10 volume fraction of Al_2O_3. The grains that protrude into the Al_2O_3 (lighter coloured phase) have curved interfaces indicating that they were taken into solution. This micrograph also illustrates that the liquid phase wets the SiC grains. The second phase can also be observed at triple points and at occasional boundaries on polished surfaces and fracture surfaces for material hot-pressed with smaller amounts (0.02 VF) of Al_2O_3. The non-dispersive X-ray attachment to the SEM only indicates the presence of Al (O is not detectable). Thus it can be concluded that a liquid phase forms at high temperatures which both wets and dissolves the SiC to promote densification by a solution-reprecipitation mechanism (e.g. [7]).

4.3. Other inhomogeneities

All dense materials contained a fine dispersion of a highly reflectant phase. Judging from their spacing, their volume fraction was ≤ 0.01. The size of these dispersed particles were rarely larger than the SiC grain size. Effort was not spent to determine their composition, but judging from the results of the X-ray diffraction analysis, they are most likely particles of

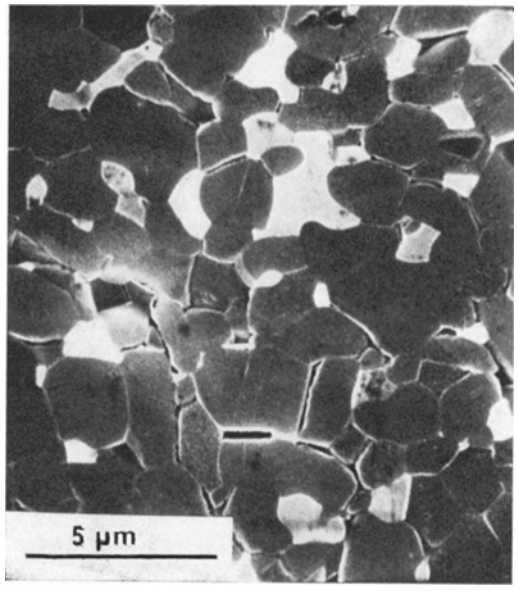

Figure 4 SEM micrograph of polished and etched section of a silicon carbide body densified with 0.10 VF Al_2O_3. Holes at boundaries are due to etching.

tungsten carbide which were incorporated during milling.

The large, non-stoichiometric SiC aggregates observed in the starting and milled PPG powders were clearly observed at fracture origins of fractured flexural bar specimens and on polished sections of this material.

Material hot-pressed at 2200°C (pressure schedule II) for 1 h with 0.02 VF Al_2O_3 contained a widely-spaced dispersion of large (> 200 μm) irregular voids, which were principally concentrated in the outer third of the disc's volume. Smaller triangular shaped voids were also observed between most of the large (> 20 μm) tabular grains. Similar large voids and significant grain growth were observed for material initially densified at 1975°C and then reheated to 2200°C for 1 h. Many of the grains in this latter material still retained their equiaxed shape and not as many smaller voids could be observed. These observations strongly suggest that the SiC and/or the Al-rich boundary phase decomposes at high temperatures to cause the formation of voids and the change of grain morphology.

Etching experiments with hot, distilled water and dilute HCl solutions did not result in any topographical changes of polished sections. This indicates that neither Al_4C_3 nor Al_4O_4C, reported to readily react with water to form methane [8], were present in the hot-pressed materials.

TABLE III Grain size of hot-pressed SiC*

Powder	Densification temperature (°C)	Volume fraction of Al_2O_3	Average grain size (μm)
EK	1950	0.02	2.0
EK	1975	0.02	3.4
EK	2025	0.02	3.7
EK	2050	0.02	4.0
EK	1975	0.10	0.7
PPG	1975	0.02	2.1
—	Norton Material	—	3.4

*Pressure schedule II.

4.4. Grain size and shape

Although the average grain size of many materials were measured using a light microscope, those listed in Table III obtained with the aid of the SEM represent more accurate values. These values are for dense material fabricated with pressure schedule II. As shown, the average grain size increases with increasing temperature. Despite the order of magnitude difference in their initial particle sizes, the PPG powder only resulted in a slightly smaller grain size relative to the EK powder. It is interesting to note that the larger amount of the Al_2O_3 hot-pressing aid resulted in a significantly smaller grain size (more than likely equivalent to the milled powder size). This is consistent with the concepts of liquid phase sintering [7], namely, when sufficient liquid is present, it separates the grains to prevent them from growing during the coalescence stage of densification. Thus, the amount of liquid (or hot-pressing aid) present has a greater effect in maintaining a small grain size relative to either the initial particle size or the hot-pressing temperature (within the reported temperature range).

At temperatures < 2100°C, an equiaxed grain morphology was obtained for material hot-pressed with the EK powder. As reported above, a large, tabular grain structure was obtained when EK powder (+ 0.02 VF Al_2O_3) was hot-pressed at 2200°C. The PPG powder (+ 0.02 VF Al_2O_3) could also result in an equiaxed microstructure, but a bimodel grain structure of small (≤ 3 μm) and large (10 to 100 μm in length) prismatic grains were also observed in several discs. The larger prismatic grains appear to be a result of exaggerated grain growth. Similar microstructures have been observed by Prochazka [9] for β–SiC powders hot-pressed with the aid of a boron additive. In one thick disc hot-pressed at 1975°C, the grain morphology changed from a bimodel, prismatic structure on one surface to an equiaxed structure on the other; its centre contained small prismatic grains. Since a small temperature gradient may have existed between the two surfaces, this observation suggests that the exaggerated grain growth phenomenon in β–SiC is sensitive to temperature.

5. Discussion

Microstructural observations clearly show that a liquid phase is responsible for the densification of SiC powder when Al_2O_3 is used as a hot-pressing aid. Although residual Al_2O_3 was identified, the composition of the liquid phase during densification is uncertain. The presence of SiO_2 and other impurities suggests the presence of an alumino-impurity-silicate phase. This is supported by the fact that densification begins at

$\sim$ 1800°C and fully dense bodies can be achieved at temperatures less than the melting point of pure Al_2O_3. Possible eutectic compositions between SiC and Al_2O_3, unknown to this author, would negate this reasoning.

The role of the liquid during densification is obvious, it allows rapid rearrangement during the initial period of pressure application and causes densification by a solution-reprecipitation mechanism. Smaller particles dissolve more rapidly resulting in greater densification rates for smaller particle size powders as reported above. The point at which coalescence and grain growth occurs is uncertain from the results reported above, but it was shown that large amounts of liquid suppresses grain growth. This is an expected result in systems that exhibit liquid phase sintering when the liquid-solid interfacial energy is greater than half the grain-boundary energy (i.e. for a dihedral angle > 0°).

Acknowledgements

The technical services of J. J. Nalevanko are sincerely appreciated. This work was supported by the Naval Air Systems Command, Contract N00019-72-C-0278.

References

1. R. A. ALLIEGRO, L. B. COFFIN and J. R. TINKLEPAUGH, *J. Amer. Ceram. Soc.* **39** (1956) 386.
2. F. G. STROKE, private communication.
3. F. F. LANGE, Naval Air Systems Command Contract N00019-72-C-0278, Final Report, April 15, 1972.
4. V. J. JENNINGS, *Mat. Res. Bull.* **4** (1969) 5199.
5. P. MURRAY, E. P. RODGERS and A. E. WILLIAMS, *Trans. Brit. Ceram. Soc.* **53** (1954) 474.
6. W. F. KNIPPENBERG, *Philips Res. Rept.* **18** (1963) 161.
7. T. S. WHALEN and M. HUMENIK, JUN, "Sintering and Related Phenomena", edited by G. C. Kuezynski, N. A. Hooton and C. F. Gibbon, (Gordon and Breach, New York, 1967) pp. 715-746.
8. L. M. FOSTER, G. LONG and M. S. HUNTER, *J. Amer. Ceram. Soc.* **39** (1956) 1.
9. S. PROCHAZKA, Naval Air Systems Command, Contract N00019-17-C-0290, Final Report, March 31, 1972.

Received 29 July and accepted 11 September 1974.